Chemical Etiology of Nucleic Acid Structure: The α-Threofuranosyl-(3′→2′) Oligonucleotide System

K.-U. Schöning, P. Scholz, S. Guntha, X. Wu, R. Krishnamurthy, A. Eschenmoser*

TNAs [(L)-α-threofuranosyl oligonucleotides] containing vicinally connected (3′→2′) phosphodiester bridges undergo informational base pairing in antiparallel strand orientation and are capable of cross-pairing with RNA and DNA. Being derived from a sugar containing only four carbons, TNA is structurally the simplest of all potentially natural oligonucleotide-type nucleic acid alternatives studied thus far. This, along with the base-pairing properties of TNA, warrants close scrutiny of the system in the context of the problem of RNA's origin.

The strategy pursued in our work to establish a chemical etiology of nucleic acid structure (*1*) demands systematic screening of the base-pairing properties of potentially natural, sugar-based nucleic acid alternatives recruited from the structural neighborhood of RNA. The β-hexopyranosyl-(6′→4′) oligonucleotide analogs of RNA (*2*) derived from the hexose sugars allose, altrose, and glucose display base pairing far inferior to that of RNA with respect to both pairing strength and pairing-mode specificity (*3*). This behavior was interpreted to be a consequence of the steric bulk of fully hydroxylated hexopyranosyl sugar units (*4*). Consequently, the focus of our studies shifted toward potentially natural RNA alternatives derived from the sterically less bulky pentopyranose sugars. There it was found that not only the pyranosyl isomer of RNA (*5*), but a whole family of diastereomeric pentopyranosyl-(4′→2′) oligonucleotide systems (*6*) show Watson-Crick base pairing that is uniformly stronger than that of RNA itself.

The RNA analogs derived from tetrose instead of pentose sugar units were not considered to be candidates, because an oligonucleotide backbone that contains six covalent bonds per repeating mononucleotide unit (as RNA does) cannot be constructed with an aldosugar containing only four carbons (*7*). However, recent observations in the pentopyranosyl series changed that perspective: switching from a (4′→2′) pentopyranosyl to a (4′→3′) pentopyranosyl system was expected to result in the loss of base pairing due to shortening the phosphodiester bridge from six to five bonds. This was observed in the β-ribopyranosyl series, but not in the α-lyxopyranosyl series (*8*). In the latter base-pairing system, the vicinal (4′→3′) phosphodiester bridge assumes a diaxial conformation at the pyranose chairs. This led us to extend our investigations to the tetrose series, because α-threofuranosyl-(3′→2′) oligonucleotides may behave as conformational analogs of α-lyxopyranosyl-(4′→3′) oligonucleotides with regard to a quasi-diaxial positioning of their phosphodiester bridge at the furanose half-chairs (Scheme 1).

Here we describe the synthesis and base-pairing properties of TNA oligonucleotides containing the five canonical purine and pyrimidine nucleobases. The tetrose-based oligonucleotides indeed show efficient base pairing which is similar to that of pentose-based RNA with regard to specificity, strand orientation, and pairing strength. In addition, TNA oligonucleotides of the L-series are capable of cross-pairing with RNA and DNA. This is in contrast to all the previously studied potentially natural nucleic acid alternatives of the (6′→4′) hexopyranosyl and the (4′→2′) pentopyranosyl families, where base pairing—in systems where it occurs—is orthogonal to that of the natural nucleic acids (*9*).

The synthesis of TNA oligonucleotides follows the methodology we used earlier in other oligonucleotide series (*4*–*6*). Starting materials **5a-e** were prepared from (L)-threose (*10*) according to Scheme 2 (*11*). All nucleosidations proceed with high diastereoselectivity to give α-nucleoside-2′,3′-dibenzoates **2a-e** in high yields. Tritylation steps **3a-e** → **4a-e** show low regioselectivity and require chromatographic separations of the major 3′-tritylated isomers from their 2′ analogs. For the thymine and uracil members **4b** and **4c**, where this separation gives the desired 3′ isomers in unsatisfactory yield, an alternative route has been developed which proceeds via intermediates **6b** and **6c** and **7b** and **7c** and produces the 3′-tritylated derivatives **4b** and **4c** selectively and in good overall yield.

X-ray structure analyses carried out on α-threofuranosyl mononucleoside derivatives containing the adenine, thymine, uracil, cytosine, or guanine nucleus (*14*) (Fig. 1) reveal a threofuranose conformation in which the two substituents at positions 2′ and 3′ indeed assume a quasi-diaxial orientation (torsion angles typically between 158° and 169°).

Table 1 summarizes the melting temperatures (T_m values) (*15*), determined by ultraviolet (UV) spectroscopy, of TNA oligonucleotide duplexes as well as the thermodynamic data for their formation from corresponding single strands (*16*). Duplex formation was also characterized by temperature-dependent circular dichroism (CD) spectroscopy, and strand stoichiometry was confirmed by UV-spectroscopic mixing curves for selected examples (Fig. 2). Base pairing in TNA strictly demands antiparallel strand orientation (Fig. 2D). Duplex stabilities show a characteristic sequence-motif dependence: Duplexes with strands composed of regularly alternating purine-pyrimidine

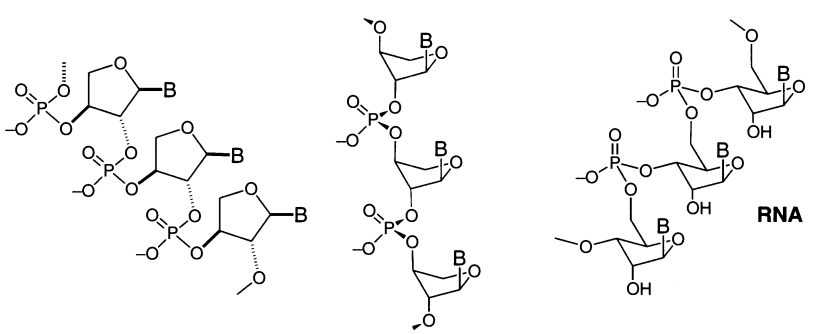

(L)-α-**THREO**-furanosyl-(**3'→2'**)-oligonucleotides ("**TNA**")

Scheme 1. Constitution, configuration, and conformation (with linearized backbone) of an (L)-α-threofuranosyl-(3′→2′) oligonucleotide strand in comparison with RNA. Equatorial substituents lie in averaged plane of pyranosyl chair, axial substituents perpendicular to it.

The Skaggs Institute for Chemical Biology at The Scripps Research Institute, 10550 North Torrey Pines Road, La Jolla, CA 92037, USA, and Laboratorium für Organische Chemie, Eidgenössische Technische Hochschule, Universitätstrasse 16, CH-8092 Zürich, Switzerland.

*To whom correspondence should be addressed. E-mail: aeschen@scripps.edu

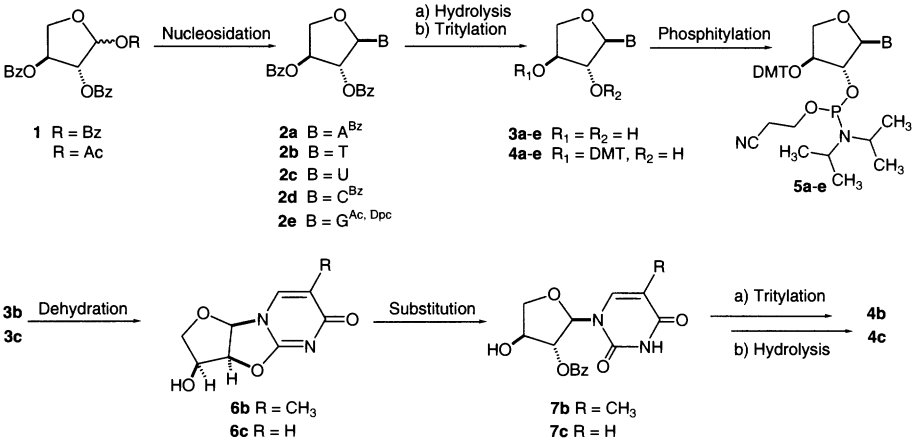

Scheme 2. Preparation of building blocks for the synthesis of (L)-α-threofuranosyl-oligonucleotides (*11*). Bz, benzoyl; Ac, acetyl; Dpc, diphenylcarbamoyl; BSA, *N,O*-bis(trimethylsilyl)acetamide; TMSOTf, trimethylsilyl trifluoromethanesulfonate; DMT, 4,4′-dimethoxy triphenylmethyl; AgOTf, silver trifluoromethane sulfonate; DMF, dimethyl formamide; HMPA, hexamethylphosphoramide; RT, room temperature. Numbers before reagents denote mole equivalents (mol-equiv.); % denotes yields of isolated products. **1** R=Bz→**2a**: 1.1 6-N-benzoyl adenine, 2.0 BSA in CH_3CN at 70°C for 1 hour, followed by 3.0 mol-equiv. $SnCl_4$ at 70°C for 1.5 hours, 91%; **1** R=Bz (**1** R=Bz, **1** R=Ac)→**2b** (**2c**, **2d**): 1.1 thymine (1.0 uracil, 1.1 4-*N*-benzoyl cytosine), 2.0 (2.2, 2.5) BSA in CH_3CN at 70°C for 1 hour, followed by 3.0 TMSOTf at 70°C for 1.5 (2, 1) hours, 92% (83, 94); **1** R=Ac→**2e**: 2-*N*-acetyl-6-*O*-diphenylcarbamoyl guanine [for method see (*12*)], 2 BSA in CH_2Cl_2 at 70°C for 1 hour, followed by 0.9 **1** R=Ac, 2 TMSOTf, in toluene at 70°C for 2.5 hours, 64%; **2a** (**2b**, **2d**, **2e**)→**3a** (**3b**, **3d**, **3e**): 2.4 (2.3, 3.3, 8) NaOH in THF/MeOH/H_2O 5:4:1, 0°C, 15 min (30, 30, 15), 85% (91, 96, 58); **2c**→**3c**: in MeOH/H_2O/Et_3N 5:1:1, reflux for 3 hours, 98%; **3a** (**3b**, **3c**, **3d**)→**4a** (**4b**, **4c**, **4d**): 1.3 DMTCl, 5 2,6-lutidine, 1.2 AgOTf in CH_2Cl_2/DMF 1:1 at 20°C for 5 (2, 5, 5) hours, followed by 0.1 (0.2, 0.1, 0.1) DMTCl, 0.1 (0.2, 0.1, 0.1) AgOTf at RT, overnight, 66% (25, 22, 45); **3e**→**4e**: 2.1 DMTCl, 6 lutidine in CH_2Cl_2/DMF 5:1 at RT for 3 days, 23%; **4a** (**4b**, **4c**, **4d**)→**5a** (**5b**, **5c**, **5d**): 1.1 P((i-Pr)$_2$N)(OCH_2CH_2CN)Cl, 5.6 ethyldiisopropylamine in CH_2Cl_2 at RT, overnight, followed by 0.1 P((i-Pr)$_2$N)(OCH_2CH_2CN)Cl for 2 hours, 64% (83, 74, 69); **4e**→**5e**: 2.5 P((i-Pr)$_2$N)(OCH_2CH_2CN)Cl, 10 *N*-ethyldimethylamine, CH_2Cl_2 at RT for 90 min, 67%. **3b** (**3c**)→**6b** (**6c**): 2.1 diphenylcarbonate, 0.3 $NaHCO_3$, HMPA at 150°C for 3 hours, 79% (92) [for method, see (*13*)]; **6b** (**6c**)→**7b** (**7c**): 4.0 BzONa, 1.1 BzOH in HMPA at 150°C for 2 hours, 68% (77); **7b** (**7c**)→**4b** (**4c**): (a) 1.5 DMTCl, 6 2,4,6-collidine in CH_2Cl_2 at RT for 16 (12) hours, 89% (96) (b) 2M NH_3 in MeOH at RT for 24 hours, 95% (93).

Table 1. T_m values (*15*) in degrees Celsius and thermodynamic data of TNA duplexes determined under conditions as follows: $c \approx 5\ \mu M + 5\ \mu M$, 1.0 M NaCl, 10 mM NaH_2PO_4, 0.1 mM Na_2EDTA, pH 7. The labels RNA and DNA refer to duplexes consisting of RNA-RNA and DNA-DNA strands, respectively. Thermodynamic parameters were determined from plots of T_m^{-1} versus ln*c* and for hairpin sequence by T_m curve differentiation at $c \approx 5.0\ \mu M$ [for methods see (*15*)]. Δ*G*, Gibbs free energy; Δ*H*, change in enthalpy (estimated experimental error for ΔH, ±5%); Δ*S*, change in entropy. For the automated synthesis of TNA-oligonucleotides see (*16*). Formation of hairpin (No. 15) is deduced from invariance of T_m (67.2° to 65.6°C) with variation in oligonucleotide concentration (2 to 111 μM).

No.	Duplex		T_m (°C) 1.0 M NaCl	T_m (°C) 0.15 M NaCl	Δ*G* (kcal/mol) (298 K)	Δ*H* (kcal/mol)	*T*Δ*S* (kcal/mol) (298 K)
1	A_8T_8		38.3		−9.2	−56.2	−47.0
2	T_8A_8		36.3		−8.6	−50.8	−42.2
3	$(TA)_8$		71.4	62	−17.4	−78.5	−61.1
4	$(AT)_8$		74.5		−18.8	−83.4	−64.6
5	$(AU)_8$		68.6	62	−20.8	−109.2	−88.4
6	$(A_2T_2)_4$		54.9		−13.7	−75.1	−61.3
7	$(A_2U_2)_4$		44.4		−12.0	−83.3	−71.3
8	$(A_4T_4)_2$		45.1		−12.8	−92.2	−79.4
9	$(A_4U_4)_2$		29.5		−7.8	−58.6	−50.8
10	$(CG)_4$		67.0		−14.6	−62.9	−48.3
11	$T(ATGC)_3ATA$		>90	84.3			
12	CGA_2T_2CG		29.8		−7.6	−41.0	−33.4
13	$(CG)_2A_2U_2(CG)_2$		69.5	68.2	−15.9*	−73.2*	−57.3*
		RNA		66.4†	−16.6†	−67.0†	−50.4†
14	$(CG)_2A_2T_2(CG)_2$		72.5	70.2	−18.1*	−82.8*	−64.7*
		DNA		58.0‡	−14.5‡	−65.2‡	−50.7‡
15	$(CG)_2T_4(CG)_2$(hairpin)		67.4		−5.0	−41.9	−36.9
16	$A_{16} + T_{16}$		42.0		−10.2	−53.6	−43.4
		RNA	62.0		−20.1	−112.4	−92.3
17	$A_{16} + U_{16}$		12.0		−5.6	−40.8	−35.2
18	$A_{20} + T_{20}$		52.6		−14.2	−75.1	−60.9
19	$A_{20} + U_{20}$		25.7		−7.9	−55.5	−47.6
20	$A_4T_3ATAT_2AT_2A + TA_2TA_2TATA_3T_4$		56.2		−14.5	−73.7	−59.2
		RNA	58.8		−20.0	−131.9	−111.9
21	$T_4A_3TATA_2TA_2T + AT_2AT_2ATAT_3A_4$		52.7		−13.3	−66.4	−53.1
		RNA	57.0		−21.8	−145.9	−124.1
22	$AT_2CAGCG + CGCTGA_2T$		31.4		−8.8	−42.2	−33.4
		RNA	52.0	46.4	−11.2*	−52.8*	−41.5*
		DNA	36.7	34.0	−9.2*	−54.4*	−45.2*

*0.15 M NaCl. †T_m value taken from (*17*); Δ*G* and *T*Δ*S* recalculated at 25°C from the original values in (*17*). ‡T_m value taken from Hunziker *et al.* (*4*) and thermodynamic values taken from (*18*).

Table 2. T_m values of duplexes A, B, C, and D formed by intra- and intersystem cross-pairing involving TNA, RNA, and DNA strands (conditions are as in Table 1). The color of the acronyms TNA, DNA, and RNA refer to the oligonucleotide sequences of the same color in the formulas of the duplexes A, B, C, and D shown at the bottom of the table. The labels 3′ and 2′ indicate strand orientation referring to TNA duplexes; for RNA and DNA duplexes, these labels must be replaced correspondingly by the labels 5′ and 3′. T_m values in the shaded diagonal refer to intrasystem cross-pairing.

	TNA	RNA	DNA	
TNA	42	28	32	A
	56	57	47	B
	53	57	43	C
	31	39	25	D
RNA	76	62	59	A
	58	59	44	B
	50	57	40	C
	41	52	36	D
DNA	68	47	55	A
	41	43	48	B
	36	41	43	C
	26	35	36	D

DUPLEX

A 3′ - A_{16} - 2′
2′ - T_{16} - 3′

B 3′ - $A_4T_3ATAT_2AT_2A$ - 2′
2′ - $T_4A_3TATA_2TA_2T$ - 3′

C 3′ - $AT_2AT_2ATAT_3A_4$ - 2′
2′ - $TA_2TA_2TATA_3T_4$ - 3′

D 3′ - ATTCAGCG - 2′
2′ - TAAGTCGC - 3′

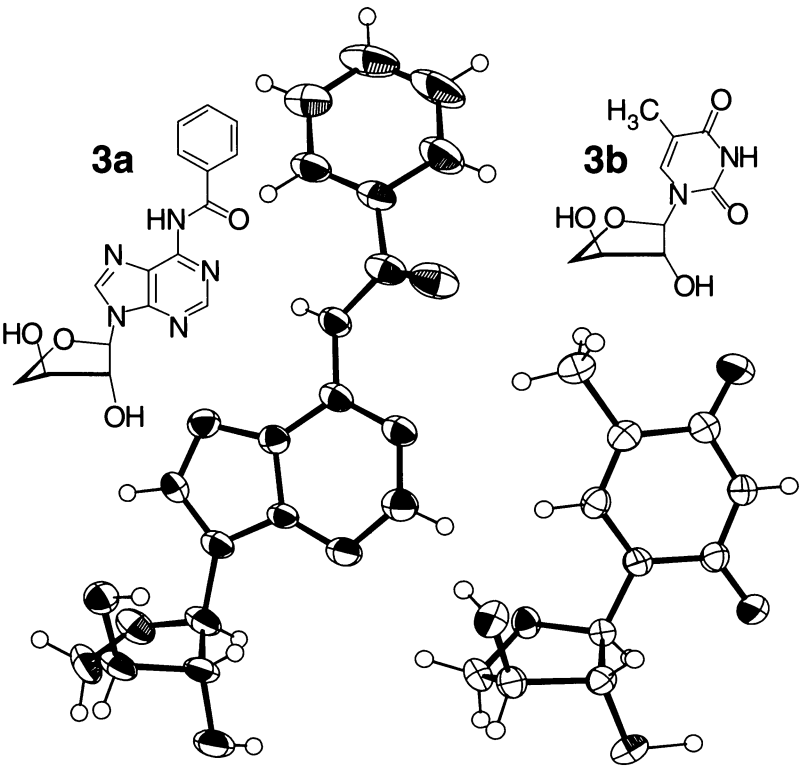

Fig. 1. X-ray structure of (L)-α-threofuranosyl nucleoside derivatives (*14*). Torsion angles (max ± 0.5 ° are as follows): O-$C_{2'}$-$C_{3'}$-O: 164.9° in **3a**, 158.6° in **3b**, 165.7° in **3c**, 2′,3′-dibenzoate, 131.5° in **3d**, 160.2° in **3e**, 2′,3′-dibenzoate. O-$C_{1'}$-N_9-C_4: −169.3° in **3a**, −176.7° in **3e**, 2′,3′-dibenzoate. O-$C_{1'}$-N_1-C_2: −147.3° in **3b**, −166.4° in **3c**, 2′,3′-dibenzoate, −169.28° in **3d**. For the chemical formula's of **3a–e**, see Scheme 2.

bases (Nos. 3, 4, and 5 in Table 1) are more stable than their isomers containing the base pairs as block oligomers (Nos. 1 and 2 in Table 1). This observation is consistent with the finding that base pairing is weakest in duplexes composed of homobasic purine and pyrimidine strands (Nos. 16 through 19 in Table 1).

With strands containing mixed purine-pyrimidine sequences of moderate length, TNA duplexes can show a thermal (but not necessarily thermodynamic) stability that is comparable to that of RNA or DNA duplexes. This is exemplified by the data for the listed duplexes (Nos. 13, 14, 20, and 21 in Table 1) and is further documented in Fig. 2 and Table 2. In contrast, base pairing of shorter oligomers (e.g., Nos. 12 and 22 in Table 1), especially when they contain homobasic sequences (e.g., No. 16 in Table 1), gives rise to duplexes that are less stable than in RNA (Table 1). Hairpins seem to form as readily in the TNA series as they do in the natural series (No. 15 in Table 1).

TNA cross-pairs efficiently with RNA and DNA. This is remarkable in view of the pronounced constitutional difference between the sugar backbones of TNA and the natural nucleic acids. The efficiency of the cross-pairing is documented by the UV melting curves and temperature-dependent CD spectra reproduced in Fig. 2, E and F, as well as by the overview of T_m values given in Table 2 for the four (non–self-complementary) base sequences A, B, C, and D. All these observations strongly suggest that the base-pairing mode of TNA is that of the Watson-Crick model.

Among the cross-pairing data is a striking characteristic difference in the behavior of homobasic versus heterobasic sequences. Whereas all intra- and intersystem combinations of the representative heterobasic hexadecamer sequences B and C give rise to comparable thermal duplex stabilities, these stabilities differ widely in corresponding combinations with the homobasic hexadecamers A_{16} and T_{16}, depending on whether the all-purine or the all-pyrimidine sequence carries the TNA backbone in the TNA-RNA heteroduplex. The T_m value of the t(A_{16}) + r(T_{16}) combination (T_m = 76°C, c = 5 + 5 μM) markedly exceeds even that of the RNA-homoduplex r(A_{16}) + r(T_{16}) (T_m = 62°C), in sharp contrast to the t(T_{16}) + r(A_{16}) combination, which is much less stable (T_m = 28°C). The same phenomenon is also observed in the cross-pairing of TNA with DNA (*20*).

Not unexpectedly, TNA is much more stable toward hydrolytic cleavage of the phosphodiester linkage than RNA; under conditions (1.0 M NaCl; 0.25 M $MgCl_2$, 0.1 M Hepes buffer, pH = 8, at 35°C) in which a half-life of about half a day was observed for r(U_8), and one of about 4 days for pyranosyl-r(T_8) (*21*), the TNA-oligonucleotide t(T_8) remains unchanged over months. TNA's stability against hydrolytic decomposition may well be similar to that of DNA (*22*).

TNA is deemed a potentially natural nucleic acid alternative according to the criteria defined earlier (*1*). In this respect, the system differs from most artificial nucleic acid analogs that also cross-pair with the natural systems, but were constructed according to the demands of antisense technology (*7*, *23*). Unlike the nucleic acid alternatives that we have studied previously, TNA could potentially serve as a template in nonenzymic template-directed formation of RNA sequences. This property remains to be experimentally tested (*24*). TNA also stands out among these alternatives—RNA included—with regard to its chemical prospects for constitutional self-assembly. The TNA structure allows for a special reactant economy in monomer formation

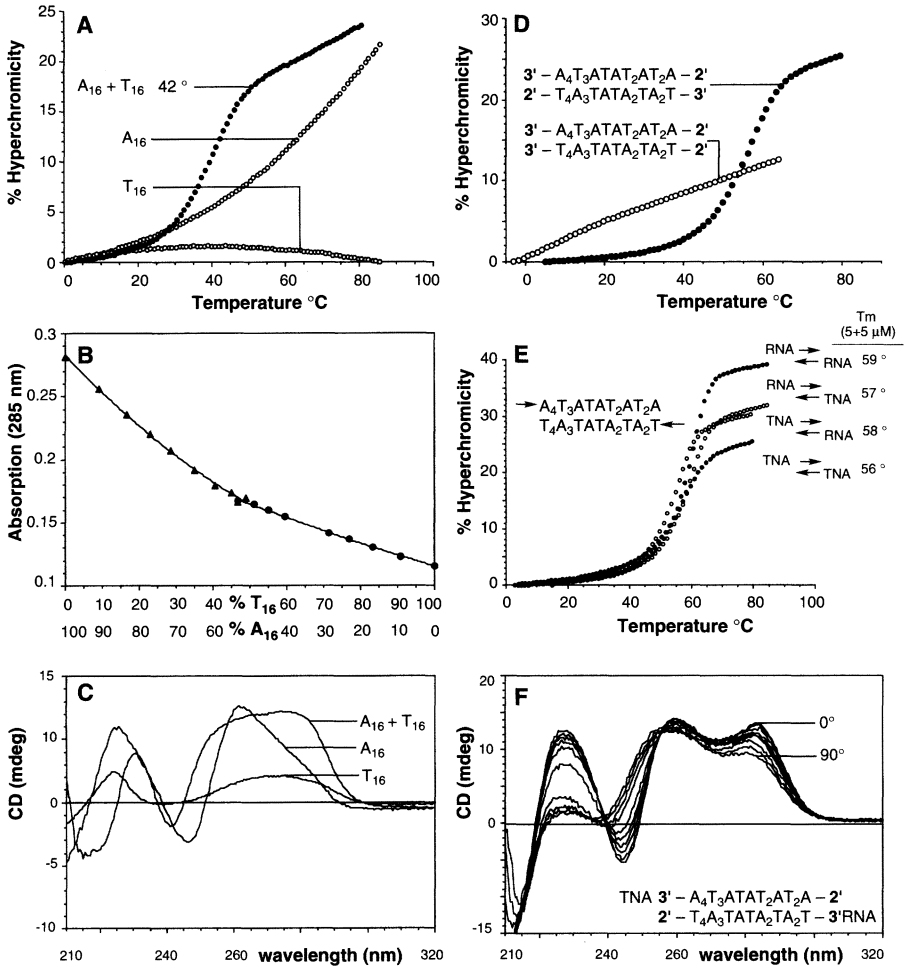

Fig. 2. Data of TNA duplexes under conditions as follows: 1.0 M NaCl, 10 mM NaH_2PO_4, 0.1 mM Na_2EDTA, pH 7. (**A**) UV melting curve of the duplex t(A_{16}) + t(T_{16}) ($c \approx 5$ μM + 5 μM), Heating curves of single strands are also shown. (**B**) Mixing curve (*19*) for the pairing between t(A_{16}) and t(T_{16}) demonstrating 1:1 stoichiometry, total $c \approx 3.6$ μM, measured at 10°C. (**C**) Comparison of CD spectra of the individual strands t(A_{16}) and t(T_{16}) and the duplex t(A_{16}) + t(T_{16}) ($c \approx 1$ μM at 30°C). (**D**) UV melting curves of (1:1)-mixtures of hexadecamer sequences complementary to each other in either antiparallel or parallel strand orientation, $c = 10$ and 20 μM, respectively. (**E**) UV melting curves and T_m values of (1:1)-mixtures of hexadecamer sequences in intra- and intersystem cross-pairing in and between TNA and RNA ($c \approx 5$ μM + 5 μM). (**F**) Temperature-dependent CD spectra of a hexadecamer duplex formed by cross-pairing between TNA and RNA ($c \approx 5$ μM + 5 μM; $T = 0°$ to 90°C).

that would have to be based on ($C_2 + C_2 \rightarrow C_4$) chemistry operating at the oxidation level of glycolaldehyde. We think that in an etiological context the full potential of such chemistry becomes apparent only if its range is not restricted to carbohydrate-phosphodiester types of target structures, but is extended to include all possible nitrogenous analogs of reactants, reactions, and reaction products (*25*). If cyanamide and cyanide were included as coreactants in such a reaction library, a whole family of potential base-pairing systems could be formed, including systems that contain alternative linkages between oligomer units, alternative nucleobases, and alternative backbone-nucleobase junctions (*26*). Thus, TNA may just be the oxygenous phosphodiester-type representative of a family of constitutionally as well as conformationally related nitrogenous systems that might all have the ability to communicate with RNA by cross-pairing. This possibility defines one direction for further experimentation (*27*).

References and Notes

1. A. Eschenmoser, in *Verh. Ges. Dtsch. Naturforsch. Aerzte*, **11b**, 135 (1990); *Science* **284**, 2118 (1999).
2. The symbol (6′→4′) indicates the phosphodiester bridges of hexopyranosyl-(6′→4′) oligonucleotides connecting the C-6′ and C-4′ carbon centers of neighboring sugar units and corresponding to the (5′→3′)-connection in RNA. The symbols (4′→2′), (4′→3′) and (3′→2′) used in this paper are to be interpreted correspondingly. They also indicate in what direction the formulas of base sequences are written.
3. R. W. Fischer, thesis, ETH Zürich (1992); A. G. Helg, thesis, ETH Zürich (1994); K. Groebke, thesis, ETH Zürich (1993); U. Diedrichsen, thesis, ETH Zürich (1993); R. Krishnamurthy, postdoctoral report, ETH Zürich (1994); A. Eschenmoser, in *Chemical Synthesis: Gnosis to Prognosis*, C. Chatgilialoglu, V. Snieckus, Eds. (Kluwer Academic, Dordrecht, Netherlands, 1996), p. 293.
4. A. Eschenmoser, M. Dobler, *Helv. Chim. Acta* **75**, 218 (1992); M. Böhringer *et al.*, *Helv. Chim. Acta* **75**, 1416 (1992); J. Hunziker *et al.*, *Helv. Chim. Acta* **76**, 259 (1993); G. Otting *et al.*, *Helv. Chim. Acta* **76**, 2701 (1993); K. Groebke *et al.*, *Helv. Chim. Acta* **81**, 375 (1998).
5. S. Pitsch, S. Wendeborn, B. Jaun, A. Eschenmoser, *Helv. Chim. Acta* **76**, 2161 (1993); S. Pitsch *et al.*, *Helv. Chim. Acta* **78**, 1621 (1995); M. Bolli, R. Micura, S. Pitsch, A. Eschenmoser, *Helv. Chim. Acta* **80**, 1901 (1997); M. Bolli, R. Micura, A. Eschenmoser, *Chem. Biol.* **4**, 309 (1997).
6. M. Beier, F. Reck, T. Wagner, R. Krishnamurthy, A. Eschenmoser, *Science* **283**, 699 (1999).
7. Homo-DNA (*4*) and pyranosyl-RNA (*5*) also contain six covalent bonds per repetitive backbone unit. The same holds for functioning nucleic acid analogs that have been made during the last decade in the context of antisense-directed oligonucleotide research. For reviews see: J. Hunziker, C. Leumann, in *Modern Synthetic Methods*, B. Ernst and C. Leumann, Eds. (Verlag Helv. Chim. Acta, Basel, Switzerland 1995), vol. 7, p. 331; P. Herdewijn, *Liebigs Ann. Chem.* **9**, 1337 (1996); B. Hyrup and P. Nielsen, *Bioorg. Chem. Med. Chem. Lett.* **4**, 5 (1996).
8. F. Reck *et al. Org. Lett.* **1**, 1531 (1999)
9. O. J. Jungmann *et al.*, *Org. Lett.* **1**, 1527 (1999).
10. The literature reports modes of forming L-threose that are not satisfactory for large scale preparation [see, e.g., K. Gätzi, T. Reichstein, *Helv. Chim. Acta* **21**, 195 (1938); M. G. López, M. S. Feather, *J. Carbohydr. Chem.* **11**, 799 (1992)]. We have developed an efficient procedure starting from (L)-ascorbic acid and will describe its details in a forthcoming publication. For an earlier synthesis of threofuranosyl-nucleosides of adenine see D. H. Murray, J. Prokop [*J. Pharm. Sci.* **56**, 865 (1967)].
11. No anomeric nucleosides were detected in the nucleosidation steps carried out under the conditions described by Vorbrüggen [H. Vorbrüggen, B. Bennua, *Chem. Ber.* **114**, 1279 (1981)]. Ratios of 3′- versus 2′-tritylated isomers isolated from the tritylation reactions strongly depended on reaction conditions and on the nature of the nucleobase. Under the conditions indicated, observed ratios were as follows: 10:1 (**4a**), 1:7 (**4b**), 1:1 (**4c**), 4:1 (**4d**), and 10:1→2:3 (**4e**). In the thymine and uracil series, intermediates **4b** and **4c** prepared via the two different routes were shown to be identical.
12. M. J. Robins, R. Zou, Z. Guo, S. F. Wnuk, *J. Org. Chem.* **61**, 9207 (1996).
13. A. V. Rama Rao, M. K. Gurjar, S. V. S. Lalitha, *J. Chem. Soc. Chem. Commun.* **10**, 1255 (1994).
14. X-ray structure analyses were carried out by B. Schweizer and R. K. Chadha. Details of these determinations will be reported in a forthcoming publication.
15. T_m is the temperature at which about half of the duplex molecules are dissociated into single strands under the conditions indicated. For definitions and methods of duplex characterization see L. A. Marky and K. J. Breslauer [*Biopolymers* **26**, 1601 (1987)].
16. Oligonucleotide sequences were synthesized on a ~1 μM scale as reported in (*5*), adopting the changes in reaction conditions as follows: coupling for 26 min using a 0.35 M solution of ethylthio-1H-tetrazole and detritylation for 10 min using a 6% dichloroacetic acid in 1,2-dichloro ethane (trityl group "on"). Coupling yields were usually over 95%. Deprotection steps before detachment from solid support were as follows: removal of β-cyanoethyl groups with NEt_3/pyridine (1:5) [room temperature (RT) for 30 min]; G-containing sequences treated additionally with 2 M *cis*-2-pyridinealdoxime in dioxane/water 7:1 (RT for 3.5 min). Detachment and nucleobase deprotection by hydrazinolysis [24% aqueous (aq.) solution at 4°C for 18 hours], followed by treatment with 80% aq. formic acid (RT for 30 min) for removal of final trityl group. Isolation, purification, and characterization of sequences were performed as reported in (*5*).
17. V. Tereshko, S. Gryaznov, M. Egli, *J. Am. Chem. Soc.* **120**, 269 (1998).
18. K. J. Breslauer, in *Thermodynamic Data for Biochem-*

istry and Biotechnology, H. J. Hinz, Ed. (Springer-Verlag, Berlin, 1986), pp. 402–427.
19. C. R. Cantor, P. R. Schimmel, *Biophysical Chemistry, Part III: The Behavior of Biological Macromolecules* (Freeman, San Francisco, 1980), pp. 1135–1139.
20. The type of "which-base-on-which-backbone" dependence of base-pairing strength encountered here seems to be a not uncommon feature of intersystem cross-pairing between complementary homobasic sequences belonging to different backbones. Although this was already apparent in the cross-pairing between RNA and DNA (Table 2) [see N. Sugimoto *et al.*, *Biochemistry* **34**, 11211 (1995); E. A. Lesnik, S. M. Freier, *Biochemistry* **34**, 10807 (1995)], it has been found to be a characteristic property of intersystem cross-pairing within the family of pentopyranosyl-(4′→2′)-oligonucleotides (*9*), and scattered literature information points to its occurrence in other combinations of base-pairing systems as well [see, e.g., M. J. Damha *et al.*, *J. Am. Chem. Soc.* **120**, 12976 (1998); A. Egger, C. Leumann, *Synlett* 913 (1999)]. Although conjectured to relate to steric differences between purines and pyrimidines in their ability to adjust nucleosidic torsion angles and, concurrently, the inclination between the backbone and base-pair axes that codetermines the topology of base-stacking (*9*), the phenomenon requires further study in order to be understood in detail.
21. T. Müller, postdoctoral report TSRI, 1998. Within the pentopyranosyl-(4′→2′) series, hydrolytic stability under these conditions parallels the occurrence of a *cis* relation between the free 3′-hydroxyl group and the adjacent phosphodiester groups.
22. In the stability tests referred to above, the DNA-sequence (T_8) was found to be completely unchanged after 8 days (monitoring was not pursued further).
23. For a recent experimental contribution to the question whether peptide nucleic acid (PNA) should be considered a potentially prebiotic type of structure see [K. E. Nelson, M. Levy, S. L. Miller, *Proc. Natl. Acad. Sci. U.S.A.* **97**, 3868 (2000); P. Garner, S. Dey, Y. Huang, *J. Am. Chem. Soc.* **122**, 2405 (2000)].
24. Studies on such template-directed synthesis of RNA oligonucleotides have recently been carried out by Orgel and colleagues [J. G. Schmidt, P. E. Nielsen, L. E. Orgel, *J. Am. Chem. Soc.* **120**, 4563 (1998); I. A. Kozlov, B. De Bouvere, A. Van Aerschot, P. Herdewijn, L. E. Orgel, *J. Am. Chem. Soc.* **121**, 5856 (1999); I. Kozler *et al.*, *Chem. Eur. J.* **6**, 151 (2000)] using Nielsen's PNA as well as Herdewijn's HNA (hexitol nucleic acid) and ANA (altritol nucleic acid) as template systems. Although the latter two are hexose-based oligonucleotides, they cannot be considered to be potentially natural nucleic acid alternatives according to the criteria given in (*1*). See also (*23*).
25. For pentofuranosyl systems with nitrogenous analogs of the phosphodiester bridge that have been shown to cross-pair with the natural systems, see [W. S. Zelinsky, L. E. Orgel, *Nucleic Acids Res.* **15**, 1699 (1987); S. M. Gryaznov *et al.*, *Proc. Natl. Acad. Sci. U.S.A.* **92**, 5798 (1995); R. O. Dempcy, O. Almarsson, T. C. Bruice, *Proc. Natl. Acad. Sci. U.S.A.* **91**, 7864 (1994); N. Kojima, T. C. Bruice, *Org. Lett.* **2**, 81 (2000)].
26. One of the persistent weaknesses of the conventional scenario for the constitutional self-assembly of a prebiotic oligonucleotide base-pairing system is the necessity of assuming a spatial and temporal separation between the nitrogenous chemistry producing the nucleobases and the oxygenous chemistry supposed to give rise to carbohydrates. Drastically enhanced chemical complications would be expected for a scenario without that separation. A hypothesis that may conceptually overcome this complication with regard to backbone formation envisages the self-assembly of an informational oligomer system to result from combinatorial synthesis proceeding under (partial) thermodynamic control. The model considers monomer- and oligomer-formation steps to operate reversibly, yet to become eventually channeled towards oligomers that possess the capability of base pairing. Such oligomers could play off their bonus in relative thermodynamic stability by making base pairing the critical selection factor in the dynamic library of oligomers. Such a fragile "thermodynamic selection" by base pairing would have to be supplemented, and eventually superseded, by the more robust selection brought about by a target system's capability to replicate. Thermodynamic functional selection (by base pairing) would appear as a forerunner of kinetic functional selection (by replication), exemplifying on the chemical level one of biology's major lessons, namely, that replication can substitute for thermodynamic stability when continuance is at stake. The model would have to imply that a constitutionally labile replicator must be able to evolve to constitutionally more robust variants by undergoing a stepwise constitutional metamorphosis while retaining the system's specific informational capacity. The high kinetic lability to be assigned to a combinatorial reaction library should not be dismissed as being a priori lethal for a model of chemical self-organization. Quite the opposite may hold in the context under consideration: kinetically labile, rather than robust, reaction libraries can be expected to possess a high sensitivity toward emerging catalysts and, therefore, a susceptibility to becoming controlled by them.
27. Supported by The Skaggs Research Foundation. K.-U.S. and P.S. thank the Deutsche Forschungsgemeinschaft and S.G. thanks the NASA/NSCORT program for fellowship support. We thank S. Pitsch (ETH) for help and advice and D. Hilvert (ETH) for critically reading the manuscript and improving the English.

21 June 2000; accepted 28 September 2000

Protection Against Cutaneous Leishmaniasis Resulting from Bites of Uninfected Sand Flies

Shaden Kamhawi,[1] Yasmine Belkaid,[1] Govind Modi,[1] Edgar Rowton,[2] David Sacks[1]*

Despite the fact that *Leishmania* are transmitted exclusively by sand flies, none of the experimental models of leishmaniasis have established infection via sand fly bites. Here we describe a reproducible murine model of *Leishmania major* infection transmitted by *Phlebotomus papatasi*. Prior exposure of mice to bites of uninfected sand flies conferred powerful protection against *Leishmania major* that was associated with a strong delayed-type hypersensitivity response and with interferon-γ production at the site of parasite delivery. These results have important implications for the epidemiology of cutaneous leishmaniasis and suggest a vaccination strategy against this and possibly other vector-borne diseases.

The diseases transmitted by arthropod vectors afflict millions of people, particularly in developing countries. Bloodsucking arthropods may be more than just delivery systems for the pathogens they carry, insofar as components in their saliva have been shown to modify the outcome of infection (*1, 2*). Leishmaniasis is a vector-borne disease transmitted exclusively by sand fly bites. Reports of successful laboratory transmission of *Leishmania* spp. by sand fly bites are few (*3–8*) and have not addressed the host response to infective bites or considered the effects of prior exposure to uninfected sand fly bites on the outcome of infection. Using the murine ear model, we were able to transmit *Leishmania major* reproducibly to BALB/c and to C57BL/6 mice (*9*) by the bite of its natural vector, *Phlebotomus papatasi* (*10*). The respective healing and nonhealing phenotypes of C57BL/6 and BALB/c mice, established using high-dose needle inocula, were maintained in fly-transmitted infections. In BALB/c mice, nodular lesions increased steadily in diameter and thickness (Fig. 1, A and B). In C57BL/6 mice, the lesions increased in size up to day 70 when they began to resolve, with complete healing by day 120 (Fig. 1, C and D). Most of the lesions developed small focalized areas of ulceration prior to healing.

In endemic regions, many individuals are exposed to the bites of *Leishmania*-free phlebotomines before being bitten by an infected sand fly. For both BALB/c and C57BL/6 mice, prior exposure to *P. papatasi* bites (*11*) resulted in a striking reduction in the severity of the dermal lesions. For BALB/c mice, the difference between naïve and pre-exposed mice was significant from days 31 and 23 onward for lesion diameter and thickness, respectively ($P < 0.05$) (Fig. 1, A and B). For C57BL/6 mice (Fig. 1, C and D), the pre-exposed animals showed a delay in the appearance of lesions and a dramatic reduction in the peak lesion size that developed before healing. The attenuation in the diameter and/or thickness of lesions was significant during days 28 to 56 ($P < 0.05$). A second transmission experiment was undertaken in naïve and pre-exposed C57BL/6 mice to compare the parasite loads within the

[1]Laboratory of Parasitic Diseases, National Institute of Allergy and Infectious Diseases, National Institutes of Health, Bethesda, MD 20892, USA. [2]Department of Entomology, Walter Reed Army Institute of Research, Washington, DC 20307, USA.

*To whom correspondence should be addressed. E-mail: dsacks@nih.gov